An Experimental Study on the Secondary Deformation of Boom Clay

Yongfeng Deng, Yu-Jun Cui, Anh Minh A.M. Tang, Xiang-Ling Li, Xavier Sillen

An Experimental Study on the Secondary Deformation of Boom Clay

Y.F. Deng[1, 2], Y.J. Cui[2], A.M. Tang[2], X.L. Li[3], X. Sillen[4]

1. Southeast University, Institute of Geotechnical Engineering, Transportation College, Nanjing, China (noden@163.com)
2. Ecole des Ponts ParisTech, Navier/CERMES, Marne-la-Vallée, France (yujun.cui@enpc.fr)
3. Euridice Group, c/o SCK/CEN, Mol, Belgium (xli@sckcen.be)
4. ONDRAF/NIRAS, Belgium (xavier.sillen@sckcen.be)

Corresponding author
Prof. Yu-Jun Cui
Ecole des Ponts ParisTech, UMR Navier/CERMES
6-8 av. Blaise Pascal, Cité Descartes, Champs-sur-Marne
F-77455 MARNE-LA-VALLEE CEDEX 2
France

E-mail: yujun.cui@enpc.fr
Tel: +33 1 64 15 35 50
Fax: +33 1 64 15 35 62

Abstract

Boom clay formation, a deposit of slightly over-consolidated marine clay that belongs to the Oligocene series in the north east of Belgium, has been selected as a possible host material of nuclear waste disposal. In this context, the long-term deformation behaviour of Boom clay is of crucial importance in the performance assessment of the whole storage system. In this study, low and high pressure oedometer tests are carried out; the e-log σ'_v (void ratio – logarithm of vertical effective stress) and e-log t (void ratio – logarithm of time) curves obtained are used to determine the compression index C_c*, swelling index C_s* and secondary deformation coefficient C_α during both loading and unloading. The relationship between C_α and the effective stress ratio (σ'_v/σ'_c, vertical effective stress to pre-consolidation stress) is analysed, and it is observed that C_α increases linearly with log $\sigma'_v/\ \sigma'_c$. Examination of the ratio of C_α/C_c* for various soils shows that the secondary deformation behaviour of Boom clay is similar to that of shake and mudstone. The relation between C_α and C_c* is linear; but the relation between C_α and C_s* is bi-linear. The bi-linearity observed is related to two different mechanisms: the mechanically dominated rebounding and the physico-chemically dominated swelling.

Keywords: Boom clay; oedometer test; secondary deformation behavior; mechanically dominated rebounding; physico-chemically dominated swelling.

1. Introduction

Boom clay formation, a thick deposit of slightly over-consolidated marine clay has been selected as a possible host material of nuclear waste disposal in Belgium. In this context, its volume change behaviour, especially its secondary deformation behaviour is essential for the safety of the whole storage system, and therefore needs to be investigated in depth.

The consolidation of fine-grained soils has been commonly described by the primary consolidation and the secondary consolidation. The former refers to the soil volume change due to water pressure dissipation whereas the latter refers to the soil volume change due to the evolution of soil fabric and soil-water interaction. In the past decades, many studies were conducted to correlate the secondary deformation coefficient (C_α) during loading with other soil characteristics. Walker (1969) showed that C_α varied with the ratio of vertical effective stress (σ'_v) to the pre-consolidation pressure (σ'_c), with the largest C_α at a stress slightly higher than σ'_c. This was confirmed by other studies on various soils (Brook and Mark, 2000; Yilmaz and Saglamer, 2004; You, 1999; Zhu *et al.*, 2005; Shirako *et al.*, 2006; Suneel *et al.*, 2008; Costa and Ioannis, 2009). Walker and Raymond (1968) found that the secondary deformation coefficient (C_α) during loading has a linear relationship with the compression index (C_c) over the full range of stress applied. This C_α-C_c relation was further investigated by many other researchers (Mesri and Castro, 1987; Mesri *et al.*, 1997; Abdullah *et al.*, 1997; Al-Shamrani, 1998; Brook and Mark, 2000; You, 1999; Feng *et al.*, 2001; Tan, 2002; Mesri, 2004; Zhang *et al.*, 2005; Zhu *et al.*, 2005; Costa and Ioannis, 2009; Feng and Zhu, 2009; Mesri and Vardhanabhuti, 2009) on various soils (intact clays, remoulded clays, clays treated with lime or cement, and sands); the results confirmed the observation by Walker and Raymond (1968). Mesri *et al.* (1994) defined four groups of soils according to the value of the ratio C_α/C_c (Table 1). Some other correlations were also attempted between C_α/C_c (or C_α) and soil physical properties such as the liquid limit w_L, plastic limit w_P and plasticity index I_p (You, 1999; Suneel *et al.*, 2008).

Although the secondary consolidation behaviour of soils has been widely investigated, there have been few studies on the stiff Boom clay, especially on the unloading path that represents the situation of the soil in vicinity of excavated galleries. In the present work, consolidation tests are performed in both low and high pressure oedometers on Boom clay taken from the sites of Essen and Mol, Belgium. Loading and unloading are run in steps and the secondary deformation coefficient C_α is determined for each step. Furthermore, the relations between C_α, the effective stress ratio (σ'_v/σ'_c), compression and swelling indexes (C_c* and C_s*) are analyzed. The main objective is to study the variations of C_α during unloading and the mechanisms involved in these variations. Note that the use of high pressure oedometer in this study allows studying the variation of C_α at large stress ratio σ'_v/σ'_c, indispensable for deeply located soil as Boom clay (223 m deep in Mol and about 240 m in Essen). Moreover, the introduction of parameter C_c* and C_s* allows analysing the soil compression behaviour with a non-linear loading-unloading curve. Note also that, to the authors' knowledge, there have been no studies before focusing on the variations of C_α during unloading.

2. Soil studied

The soil studied was taken by coring at the sites of Essen and Mol, Belgium. The location of the two sites is shown in Figure 1 (De Craen *et al.*, 2006). The Essen site is situated in the north east of Belgium, about 60 km far from the underground research laboratory (URL) at the Mol site. After being taken from the borehole, the cores were sealed in plastic tubes having ends closed and transported to the laboratory. Five soil cores of 1-m length and 100-mm in diameter from Essen and one soil core of 0.5-m length and 100-mm in diameter from Mol were studied. The details of these cores are shown in Table 2, with the corresponding depth, member, unit mass of solids (ρ_s), liquid limit (w_L), plastic limit (w_P), plasticity index (I_p), water content (w_0) and void ratio (e_0). There are three cores taken from the Putte member (Mol, Ess75 and Ess83) and three cores from the Terhagen members (Ess96, Ess104 and Ess112). The geotechnical identification parameters of the cores from Essen are similar: ρ_s = 2.64 – 2.68; w_L = 62 – 78%; w_P = 25 – 33%; I_P = 36 – 45. The values are also close for both water content and void ratio: w_0 = 27.2 – 29.7, e_0 = 0.700 – 0.785. For the core from Mol, the values of ρ_s, w_L, w_P and I_P are similar to that of the cores from Essen, but the water content and void ratio are lower than the cores from Essen, showing that Boom clay from Mol is denser.

3. Experimental techniques

Both low pressure (0.05 - 3.2 MPa) and high pressure (0.125 - 32MPa) oedometer tests were carried out following the French standards (AFNOR 1995, 2005) on the six Boom clay cores. The tests in low pressure oedometer aim at studying the loading-unloading behavior of the soil near the excavation gallery, whereas the tests in high pressure oedometer aim at studying the compression behavior in large stress level (far from the excavation gallery). The soil samples were prepared by trimming and had 50-mm in diameter and 20-mm in height. In the following, high pressure oedometer test is named Oedo1 while low pressure test is named Oedo2. Note that the high pressure oedometer has the same principle as the standard low pressure oedometer; the main difference is that in high pressure oedometer two amplification levels were used with a ratio of 1:10 for the first level and 1:5 for the second level (see Figure 2). In other words, the frame of high pressure oedometer allows multiplying the applied weight by 50, which leads to a maximum force of 12 tons. In the experiments, the minimum and maximum applied weights are 5 N and 1280 N, leading to a minimum and maximum vertical pressure of 0.125 MPa and 32 MPa respectively for a sample of 50 mm diameter.

The soil specimen was installed in the cell with dry porous stones. Prior to circulation of the synthetic water which has the same chemistry as the in-situ pore water (Cui *et al.*, 2009) in the drainage system, a confining pressure equal to the estimated in situ stress was applied. This prevents the soil swelling during re-saturation which may modify the soil microstructure and as a result the soil mechanical properties (Delage *et al.*, 2007).

The in situ stress of the soil was estimated using Eq. 1:

$$\sigma'_{v0} = \gamma h - u_0 \quad (1)$$

where σ'_{v0} is the in situ effective vertical stress; γ is the mean unit weight of the soil above the depth considered, taken equal to 20 kN/m^3 following the data of De Craen *et al.* (2006); *h* is

the depth of the soil core (see Table 2); u_0 is the in situ pore pressure estimated from the ground water level that is assumed to be at the ground surface. The σ'_{v0} values determined for Ess75, Ess83, Ess96, Ess104, Ess112 and Mol are 2.20, 2.27, 2.40, 2.48, 2.56 and 2.23 MPa, respectively. For a reason of convenience, σ'_{v0} in both low pressure and high pressure oedometers was set at 2.40 MPa for all tests.

4. Experimental results

4.1. Compressibility behavior

Figure 3 presents the loading-unloading-reloading stages and the corresponding changes in vertical displacement in test Ess75Oedo1. Before the re-saturation phase, a loading from 0.125 to 2.4 MPa was applied to reach the in situ stress state. The soil sample was then re-saturated using synthetic water. The subsequent unloading-reloading stages were as follows: unloading from point A (2.4 MPa) to B (0.125 MPa); loading to C (16 MPa); unloading to D (0.125 MPa); loading to E (32 MPa) and unloading to F (0.125 MPa). Common results were obtained in terms of vertical displacements, *i.e.* compression upon loading and rebounding upon unloading. Note that the French standards – AFNOR (1995, 2005) were applied as regards the deformation stabilization for all odometer tests: stabilization is achieved when the displacement rate is lower than 0.01mm/h.

Figure 4 presents the compression curve (void ratio versus $\log\sigma'_v$) of test Ess75Oedo1, together with the compression curve of test Ess75Oedo2 in low pressure odometer. In test Ess75Oedo2, after the re-saturation using synthetic water under 2.4 MPa stress, unloading was performed from point I (2.4 MPa) to point II (0.05 MPa), then loading to point III (3.2 MPa) and finally unloading to point IV (0.05 MPa).

The low pressure oedometer test Ess75Oedo2 shows a quasi elastic behavior with narrow unloading-loading loops. A deeper examination shows, however, that the reloading curve from II to III is not linear in the plane e-log σ'_v. This non-linearity can be also observed on the curve of test Ess75Oedo1 on the reloading paths from B to C and from D to E. Note that the results from the tests on other cores are similar to that shown in Figure 4. Obviously, it is difficult to determine the pre-yield stress σ'_y using the Casagrande method on these curves. In addition, this pre-yield stress, if any, does not correspond to the pre-consolidation pressure σ'_c (σ'_y is much lower than σ'_c): σ'_c is equal to 2.4 MPa at point A, but when reloading from B to C, σ'_y seems to be much lower, about 1 MPa. For this reason, in the following analysis only σ'_c is used and its determination is based on the stress history: σ'_c is the maximum stress applied in the oedometer tests. For instance, σ'_c = 16 MPa for the paths C->D and D->E; σ'_c = 32 MPa for the path E->F; σ'_c = 3.2 MPa for the path III->IV is 3.2 MPa.

Since the e-log σ'_v curves of Boom clay are not linear during unloading and unloading, especially for the low pressure oedometer tests, it is difficult to use an unique compression index (C_c) and swell index (C_s) to describe the compression and swelling behavior. Hence the above two indexes are determined stage by stage, and renamed C_c* and C_s*, respectively. It should be pointed out that if the e-log σ'_v curves for the three stages (*i.e.* before pre-yielding, after pre-yielding and unloading) are linear, the C_c* becomes the same as C_c and C_s* becomes the same as C_s.

For the determination of secondary deformation coefficient C_α, standard method is used

based on the e - Δlog *t* plot. The determination of C_c*, C_s* and C_α is illustrated in Figure 5. Note that $C_\alpha = \Delta e/\Delta \log t$ is negative when loading and positive when unloading.

4.2. Relation between C_α and σ'_v/σ'_c

Figure 6 shows the variation of C_α versus the stress ratio σ'_v/σ'_c for all the six cores, identified by both low pressure and high pressure oedometer tests. It appears that during loading stage C_α ranges mostly from 0 to 0.01 especially when the vertical effective stress is lower than the pre-consolidation stress. Some points beyond 0.01 can be observed when the stress ratio is greater than 2. For core Ess112, C_α is very small and close to zero when the stress ratio is less than 1. For the unloading stages, C_α ranges mostly from 0 to -0.01 for all tests when the stress ratio is greater than 0.1. On the contrary, when the stress ratio is less than 0.1, C_α is less than -0.01. These observations lead to conclude that more significant secondary consolidation takes place at higher stress ratios ($\sigma'_v/\sigma'_c > 1$) upon loading and more significant secondary swelling takes place at lower stress ratios ($\sigma'_v/\sigma'_c < 0.1$).

Except the results of core Ess112 during loading, all other results show that C_α increases almost linearly with the stress ratio in the semi-logarithmic plane, for both loading and unloading stages. This is different from the results reported by other authors (Walker, 1969; Brook and Mark, 2000; Yilmaz and Saglamer, 2007; You, 1999; Zhu *et al.*, 2005; Shriako *et al.*, 2006; Suneel *et al.*, 2008; Costa and Ioannis, 2009) who observed that the relation between C_α and log σ'_v/σ'_c during loading is rather convex.

4.3. Relation between C_c* or C_s* and C_α

Figure 7 shows the variations of C_α with C_c* and C_s* for all the cores. It appears that C_α increases linearly with C_c*, with a slope ranging from 0.019 to 0.029. Moreover, this linear relation is independent of the state of consolidation: for a given core, all the points below and beyond σ'_c are on the same line.

Mesri *et al.* (1994) analyzed the secondary consolidation behaviour of many soils, and gave the correlation between the secondary consolidation coefficient (C_α) and the compression index C_c as shown in Table 1. From the results obtained on Boom clay, it appears that the ratio C_α/C_c* falls in a narrow range from 0.019 to 0.029. In order to have a mean value, all the results during loading are gathered in Figure 8, in terms of variations of C_α versus C_c*. A value of 0.024 is identified for the ratio C_α/C_c*. Based on the classification criterion in Table 1, one can conclude that Boom clay falls in the zone of shake and mudstone whose C_α/C_c* value ranges from 0.02 to 0.04.

Figure 7 also shows that during unloading, a bi-linear relation between C_α and C_s* can be observed: the turning point at a C_s* value around 0.1. This turning point can be considered as an indicator of changes from mechanical dominance to physical-chemical dominance in terms of volume changes: when C_s* is less than the value at the turning point, the clay shows a mechanically dominated rebounding; by contrast, when C_s* is larger than the value at the turning point, the clay shows a physico-chemically dominated swelling. This particular behaviour during unloading was also observed in other works: Delage *et al.* (2007) and Le *et al.* (2011) conducted compression tests on unsaturated Boom clay with suction monitoring, and observed that during unloading the soil suction increased slowly in the beginning and then rapidly when the vertical stress decreased down to a threshold value; Cui *et al.* (2002)

observed that the microstructure of a compacted bentonite/sand mixture started to change much more drastically when the suction was lower than 1 MPa; Cui *et al.* (2008) and Ye *et al.* (2009) observed that the unsaturated hydraulic behaviour of compacted bentonite-based materials under confined conditions changed drastically when the suction was lower than a threshold value.

All the data of C_α versus C_s* are gathered in Figure 9. In spite of the significant scatter, a bilinear relation can be still identified, with -0.024 and -0.26 as slopes. It is interesting to note that the absolute value of the slope of the first part (where the volume change behavior is supposed to be governed by the mechanical effect) is equal to the value of C_α/C_c* during loading (0.024). This observation confirms that the first part of unloading (C_s* < 0.1) gives rise to a mechanically dominated rebounding, because the volume change behavior during loading can be regarded as governed by the mechanical effects. The larger slope of the second part (0.26, when C_s* > 0.1) indicates a significant secondary swelling behavior compared to the mechanical secondary consolidation behavior.

5. Conclusion

Both low pressure and high pressure oedometer tests were carried out with loading and unloading on Boom clay samples taken by coring from Essen and Mol sites. The *e*-log σ'_v and e-log *t* curves were plotted to determine the compression index C_c*, swell index C_s* and secondary deformation coefficient C_α. Note that C_α was determined for either loading stages (secondary consolidation) or unloading stages (secondary swelling). Different relations such as $C_\alpha - \sigma'_v/\sigma'_c$, $C_\alpha - C_c$*, and $C_\alpha - C_s$* were analyzed. The following conclusions can be drawn:

(i) C_α increases almost linearly with the stress ratio σ'_v/σ'_c in the semi-logarithmic plane, for both loading and unloading stages. This linear relation during loading was different from that observed by other researchers who concluded rather a convex relation for other soils.

(ii) C_α increases linearly with C_c*, with a slope of 0.024. In addition, this linear relation is independent of the state of consolidation. During unloading, a bi-linear relation between C_α and C_s* was identified, with the turning point at a C_s* value around 0.1 and the values of slopes of -0.024 and -0.26, respectively.

(iii) The two slopes of the C_α - C_s* curve relate to two different mechanisms: the first part (C_s* < 0.1) relates to a mechanically dominated rebounding whilst the second part (C_s* > 0.1) relates to a physico-chemically dominated swelling. This observation was confirmed by the equality of the slopes for the first unloading part and the loading part (0.024), because the volume change behavior during loading can be regarded as governed by the mechanical effects.

(iv) According to the classification criterion defined by Mesri *et al.* (1994), Boom clay falls in the zone of shake or mudstone whose C_α/C_c* value ranges from 0.02 to 0.04.

Acknowledgements

ONDRAF/NIRAS (The Belgian Agency for Radioactive Waste and Enriched Fissile Materials)

is greatly acknowledged for its financial support. The first author is grateful to the National Science Foundation of China for its support (No 50908049).

References:

Abdullah, W.S., Al-Zoubi, M.S. and Alshibli, K.A. 1997. On the physicochemical aspects of compacted clay compressibility. Canadian Geotechnical Journal 34, 551–559.

AFNOR, 1995. Sols : reconnaissance et essais: essai de gonflement à l'oedomètre, détermination des déformations par chargement de plusieurs éprouvettes. XP P 94-091.

AFNOR, 2005. Geotechnical investigating and testing, Laboratory testing of soils, Part 5: Incremental loading odometer test. XP CEN ISO/TS 17892-5.

Al-Shamrani, M., 1998. Application of the C_α/C_c concept to secondary compression of Sabkha soils. Canadian Geotechnical Journal 35, 15-26.

Brook, E. and Mark A. A. 2000. Secondary compression of soft clay from Ballina. Proc. GeoEng 2000, Melbourne, Australia.

Costas, A.A. and Ioannis, N.G. 2009. A new model for the prediction of secondary consolidation index of low and medium plasticity clay soils. European Journal of Scientific Research 34(4), 542-549.

Cui, Y.J., Loiseau, C. and Delage, P. 2002. Microstructure changes of a confined swelling soil due to suction controlled hydration. Proc. of the Third Inter. Conf. on Unsaturated Soils UNSAT2002, Recife, vol. 2, 593-598.

Cui, Y.J., Tang, A.M., Loiseau, C. and Delage, P. 2008. Determining the unsaturated hydraulic conductivity of a compacted sand-bentonite under constant-volume and free-swell conditions. Physics and Chemistry of the Earth 33, S462-S471.

Cui, Y.J., Le, T.T., Tang, A.M., Delage, P., and Li, X.L. 2009. Investigating the time dependent behavior of Boom clay under thermomechanical loading. Géotechnique 59(4), 319-329.

De Craen, M., Wemaere, I., Labat, S., and Van Geet, M. 2006. Geochemical analyses of Boom Clay pore water and underlying aquifers in the Essen-1 borehole. External report, SCK.CEN-ER-19, 06/MDC/P-47, Belgium

Delage, P., Le, T.T., Tang, A.M., Cui, Y.J., and Li, X.L. 2007. Suction effects in deep Boom clay samples. Géotechnique 57(2), 239-244.

Feng, T.W., Lee, J.Y. and Lee, Y.J. 2001. Consolidation behavior of a soft mud treated with small cement content, Engineering Geology 59, 327-335.

Feng, Z.G., and Zhu, J.G. 2009. Experimental study on secondary behavior of soft clays. Journal of Hydraulic Engineering 40(5), 583-588 (In Chinese).

Le, T.T., Cui, Y.J., Munoz, J.J., Delage, P. and Li, X.L. 2011. Studying the hydraulic and mechanical coupling in Boom clay using an oedometer equipped with a high capacity tensiometer. Frontier of Architecture and Civil Engineering in China 5(2), 160-170.

Mesri, G., and Castro, A. 1987. The C_α/C_c concept and Ko during secondary compression. Journal of Geotechnical Engineering Division 112(3), 230-247.

Mesri, G., Kwan, L.D.O., and Feng, W.T. 1994. Settlement of embankment on soft clays. Proc. Of settlement 94, ASCE GSP 40, 8-56.

Mesri, G., Stark, T. D., Ajlouni, M. A., and Chen, C. S. 1997. Secondary compression of peat with or without surcharging. Journal of the Geotechnical Engineering Division 123(5), 411-421.

Mesri, G., 2004. Primary compression and secondary compression, Proc. of Soil Behavior and Soft Ground Construction, ASCE GSP 119, 122-166.

302 Mesri, G. and Vardhanabhuti, B. 2009. Compression of granular materials. Canadian
303 Geotechnical Journal 46, 369–392.
304 Shriako, H., Sugiyama, M., Tonosaki, A. and Akaishi, M. 2006. Secondary compression
305 behavior in standard consolidation tests. Proc. of Schl. Eng, Tokai University 31, 27-32
306 Suneel, M., Park, L.K., and Chulim J. 2008. Compressibility characteristics of Korean marine
307 clay. Marine Georesources and Geotechnology 26, 111–127.
308 Tan, Z.H., 2002. The behavior of compression and consolidation for clays. These of Taiwan
309 Central University, China, 428 pp. (In Chinese).
310 Walker, L.K. and Raymond, G.P. 1968. The prediction of consolidation rates in a cemented
311 clay. Canadian Geotechnical Journal 5(4), 192-216.
312 Walker, L.K., 1969. Secondary settlement in sensitive clays. Canadian Geotechnical Journal
313 6(2), 219-222.
314 Ye, W.M., Cui, Y.J., Qian, L.X., Chen, B. 2009. An experimental study of the water transfer
315 through compacted GMZ bentonite. Engineering Geology 108, 169 – 176.
316 Yilmaz, E. and Saglamer A. 2007. Evaluation of secondary compressibility of a soft clay. The
317 bulletin of the Istanbul Technical University 54 (1), 7-13.
318 You, M.Q., 1999. Compression and consolidation behavior under different sampling, loading
319 methods. Thesis of Taiwan Central University, China, 124 pp. (In Chinese).
320 Zhang, J.H., Miao, L.C. and Huang, X.M. 2005. Study on secondary consolidation
321 deformation of soft clay. Journal of Hydraulic Engineering 36(1), 1-5 (In Chinese).
322 Zhu, H.H, Chen, X.P., Zhang F.J. and Huang, L.J. 2005. Consolidation behaviors of soft soil
323 in Nansha, Geotechnical Investigation and Surveying 33(1), 1-3 (In Chinese).

List of Tables

Table 1. Soil classification according to the values C_α/C_c (Mesri *et al.*, 1994)
Table 2. Geotechnical properties of the soil cores studied

List of Figures

Figure 1. Locations of the sampling sites (De Craen *et al.*, 2006)
Figure 2 Sketch of high pressure oedometer
Figure 3. Vertical effective stress and displacement versus elapsed time (Ess75Oedo1)
Figure 4. Compression curves from oedometer tests (Ess75Oedo1 and Ess75Oedo2)
Figure 5. Determination of parameters C_c*, C_s* and C_α
Figure 6. C_α versus stress ratio σ'_v/σ'_c. (a) Core Ess75; (b) Core Ess83; (c) Core Ess96; (d) Core Ess104; (e) Core 112; (f) Core Mol
Figure 7. C_α versus C_c* and C_s*. (a) Core Ess75; (b) Core Ess83; (c) Core Ess96; (d) Core Ess104; (e) Core 112; (f) Core Mol
Figure 8. C_α versus C_c*
Figure 9. C_α versus C_s*

340

341 Table 1. Soil classification according to the values C_α/C_c (Mesri *et al.*, 1994)

Material	C_α/C_c
Granular soils including rockfill	$C_\alpha/C_c = 0.02 \pm 0.01$
Shake and mudstone	$C_\alpha/C_c = 0.03 \pm 0.01$
Inorganic clays and silts	$C_\alpha/C_c = 0.04 \pm 0.01$
Organic clays and silts	$C_\alpha/C_c = 0.05 \pm 0.01$
Peat and muskeg	$C_\alpha/C_c = 0.06 \pm 0.01$

342

343

344 Table 2. Geotechnical properties of the soil cores studied

Core	Depth (m)	Member	ρ_s (Mg/m^3)	w_L (%)	w_p (%)	I_p (%)	w_0 (%)	e_0
Ess75	218.91-219.91	Putte	2.65	78	33	45	29.7	0.785
Ess83	226.65-227.65	Putte	2.64	70	33	37	27.2	0.730
Ess96	239.62-240.62	Terhagen	2.68	69	33	36	26.5	0.715
Ess104	247.90-248.91	Terhagen	2.68	68	29	39	27.7	0.700
Ess112	255.92-256.93	Terhagen	2.67	62	25	37	27.3	0.755
Mol	223	Putte	2.67	68	26	42	23.6	0.625

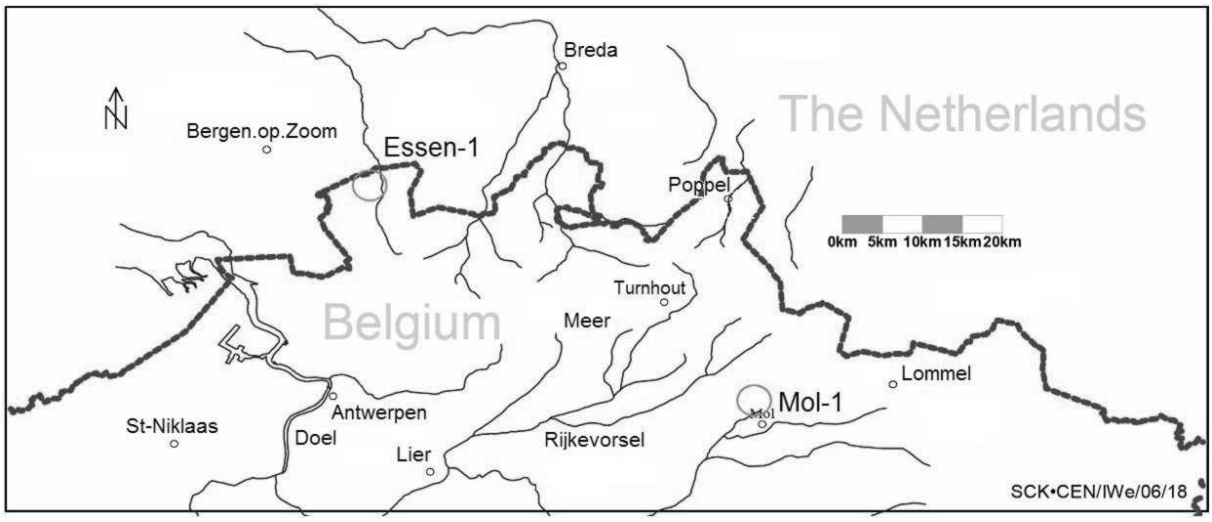

345

346 Figure 1. Locations of the sampling sites (De Craen *et al.*, 2006)

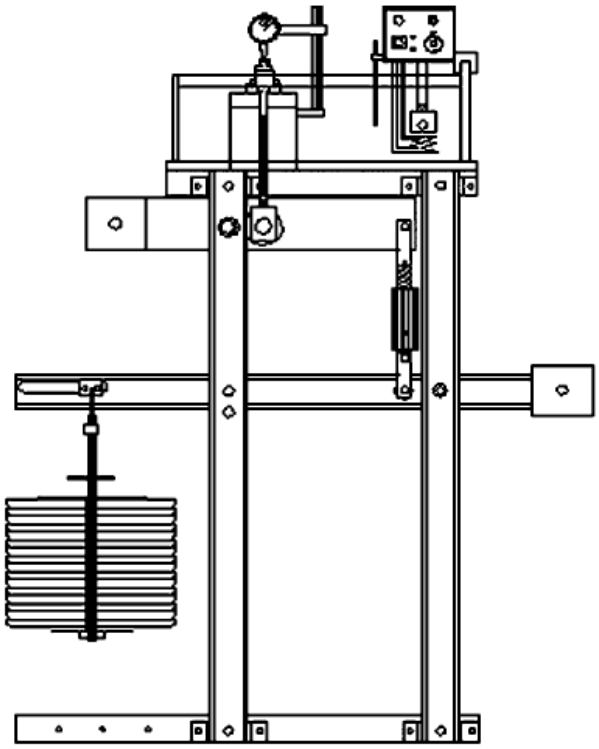

Figure 2 Sketch of high pressure oedometer

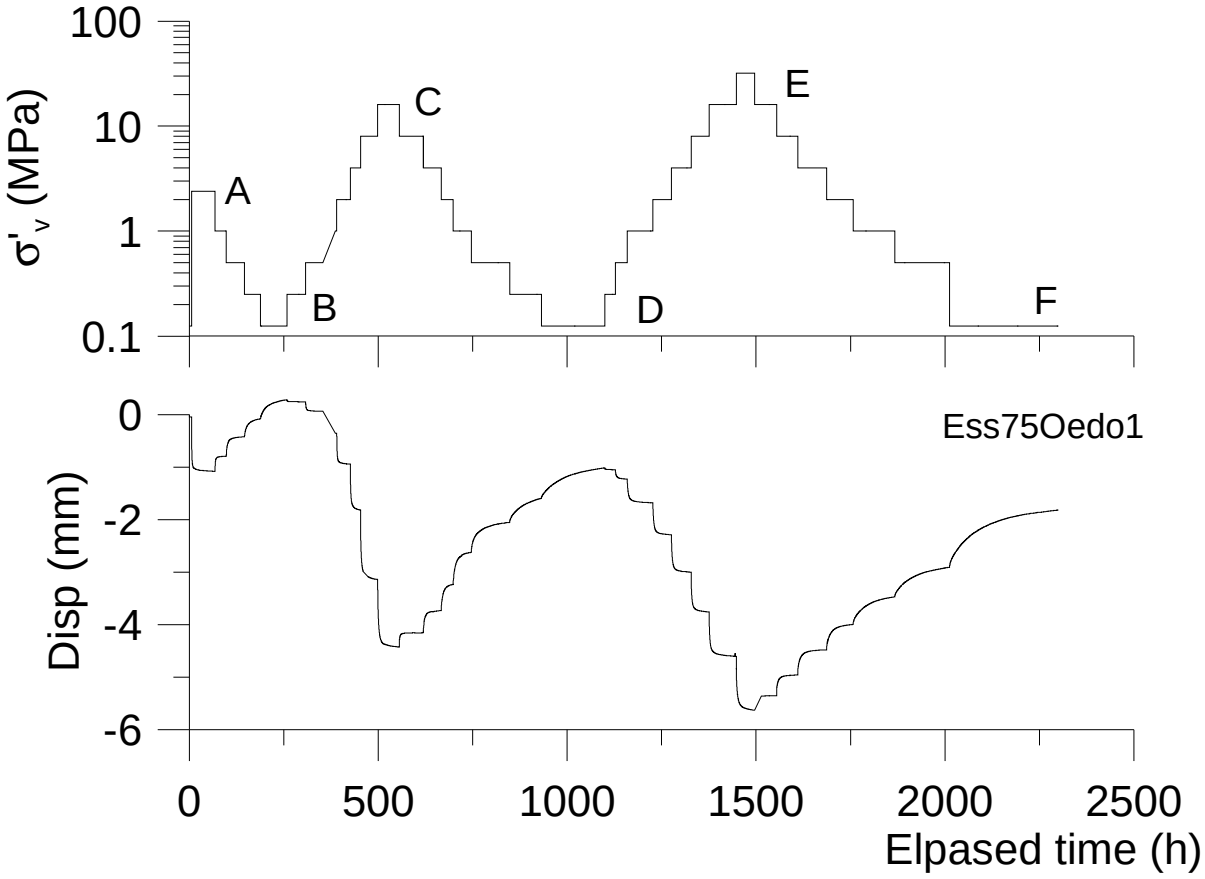

Figure 3. Vertical effective stress and displacement versus elapsed time (Ess75Oedo1)

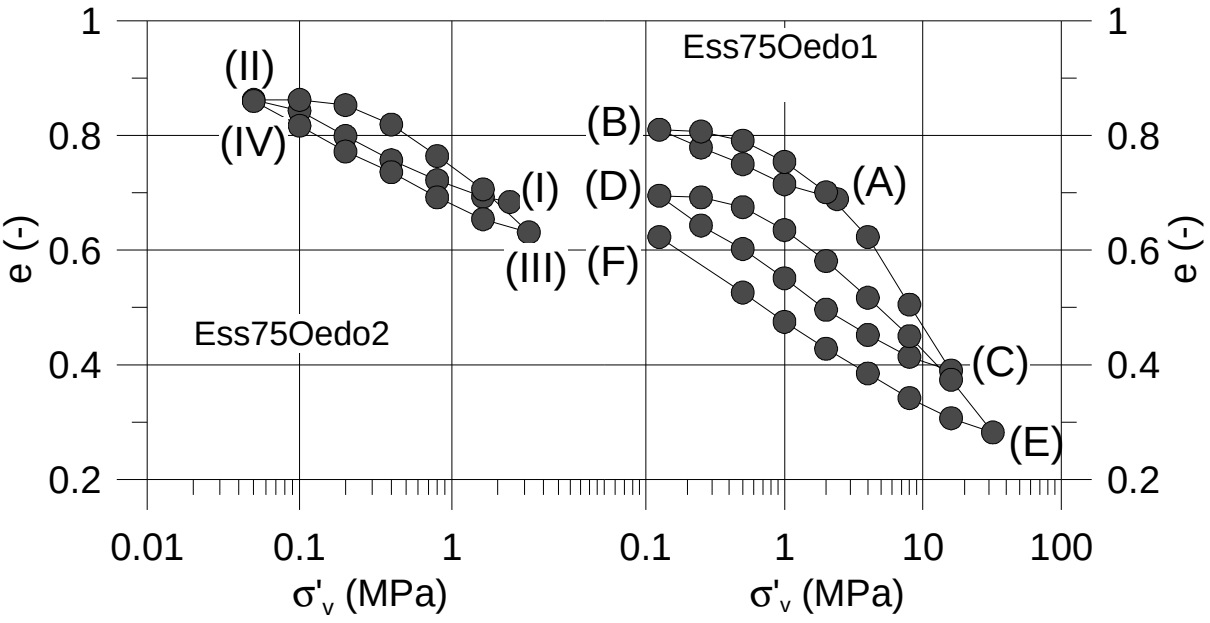

Figure 4. Compression curves from oedometer tests (Ess75Oedo1 and Ess75Oedo2)

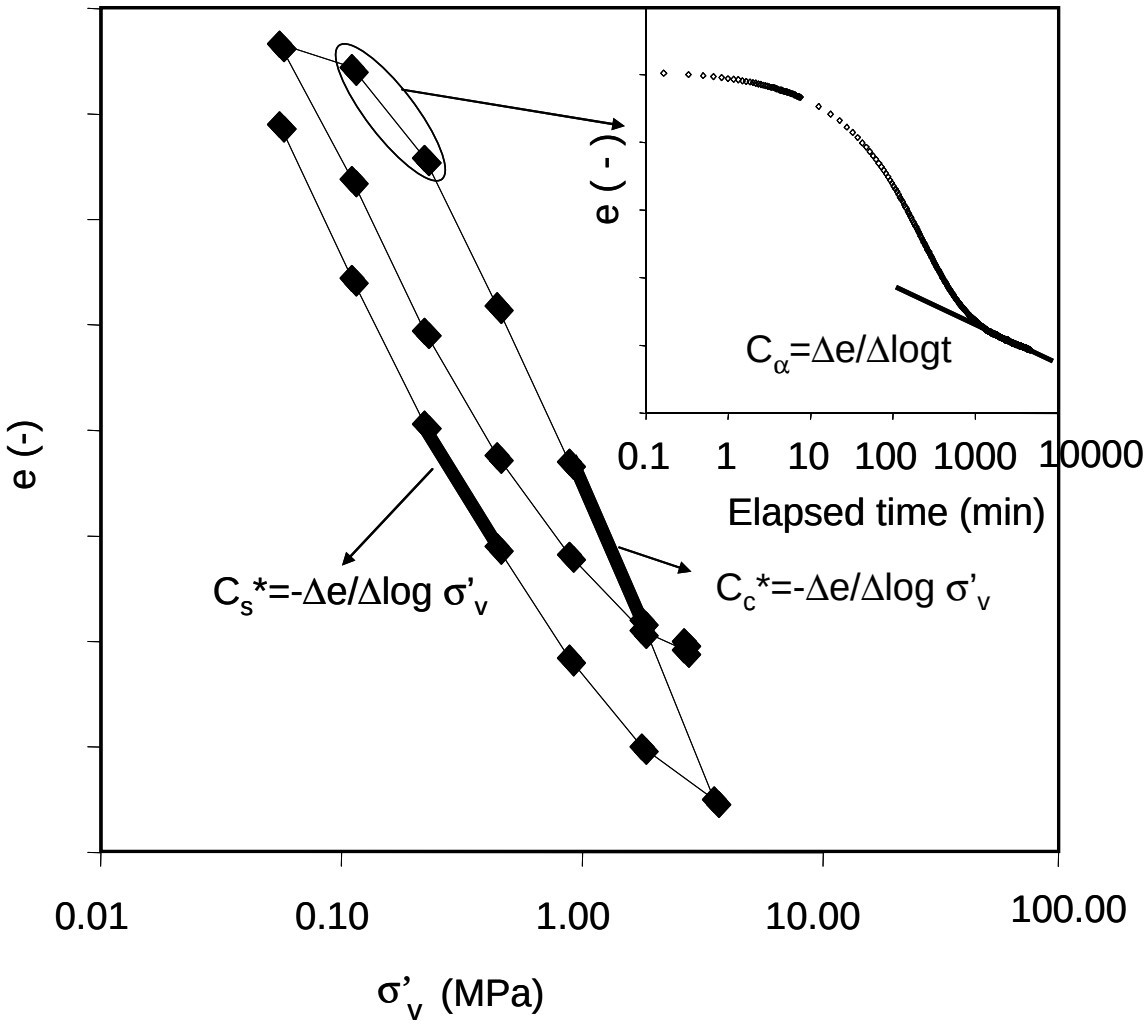

Figure 5. Determination of parameters C_c*, C_s* and C_α

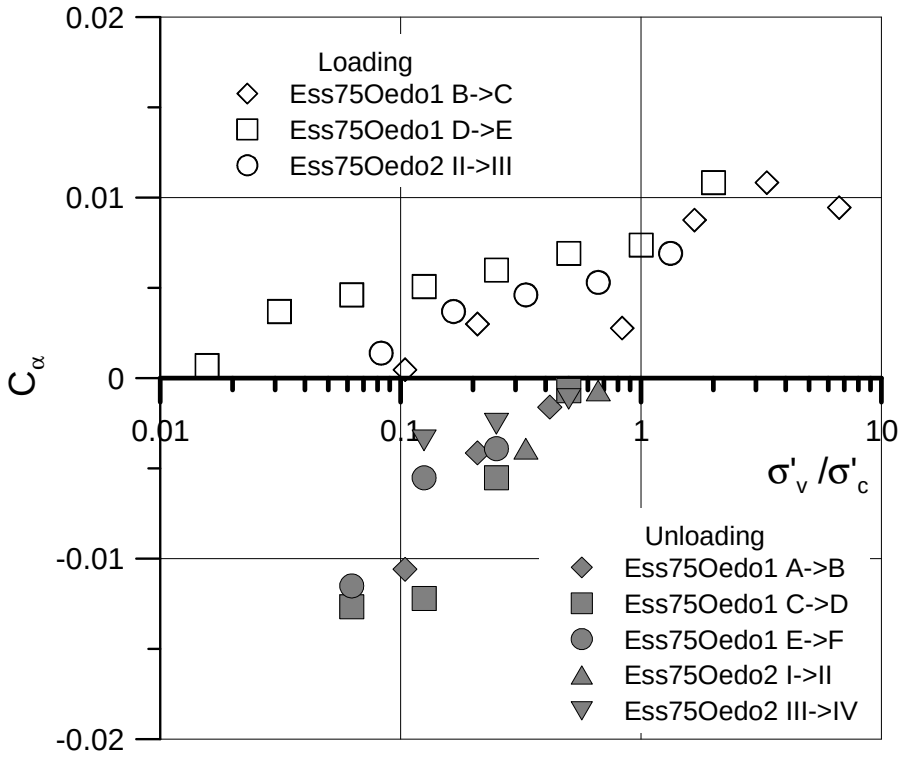
0.02
0.01
0
-0.01
-0.02
0.01
0.1
1
10
C_α
σ'_v / σ'_c
Loading
Ess75Oedo1 B->C
Ess75Oedo1 D->E
Ess75Oedo2 II->III
Unloading
Ess75Oedo1 A->B
Ess75Oedo1 C->D
Ess75Oedo1 E->F
Ess75Oedo2 I->II
Ess75Oedo2 III->IV

(a)

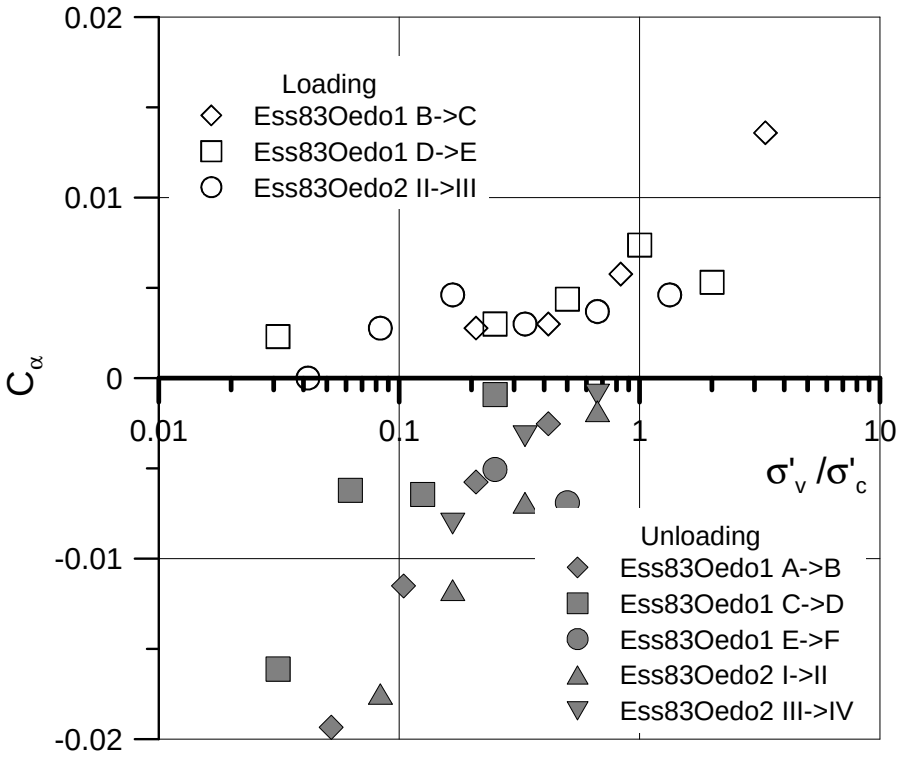
0.02
0.01
0
-0.01
-0.02
0.01
0.1
1
10
C_α
σ'_v / σ'_c
Loading
Ess83Oedo1 B->C
Ess83Oedo1 D->E
Ess83Oedo2 II->III
Unloading
Ess83Oedo1 A->B
Ess83Oedo1 C->D
Ess83Oedo1 E->F
Ess83Oedo2 I->II
Ess83Oedo2 III->IV

(b)

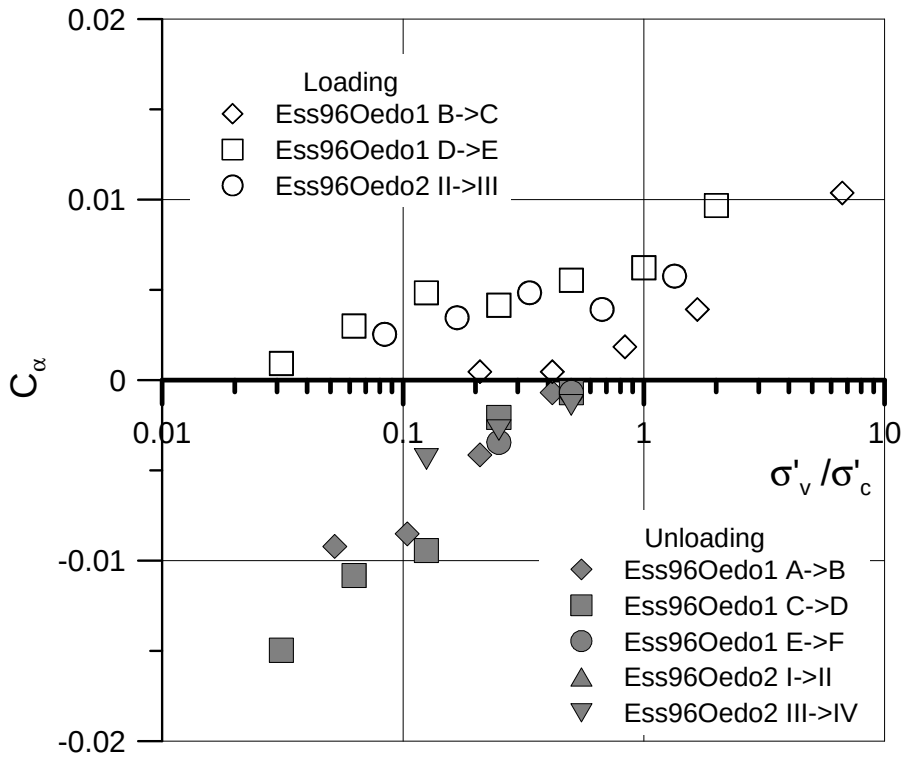
0.02
0.01
0
-0.01
-0.02
0.01
0.1
1
10
C_α
σ'_v/σ'_c
Loading
Ess96Oedo1 B->C
Ess96Oedo1 D->E
Ess96Oedo2 II->III
Unloading
Ess96Oedo1 A->B
Ess96Oedo1 C->D
Ess96Oedo1 E->F
Ess96Oedo2 I->II
Ess96Oedo2 III->IV

(c)

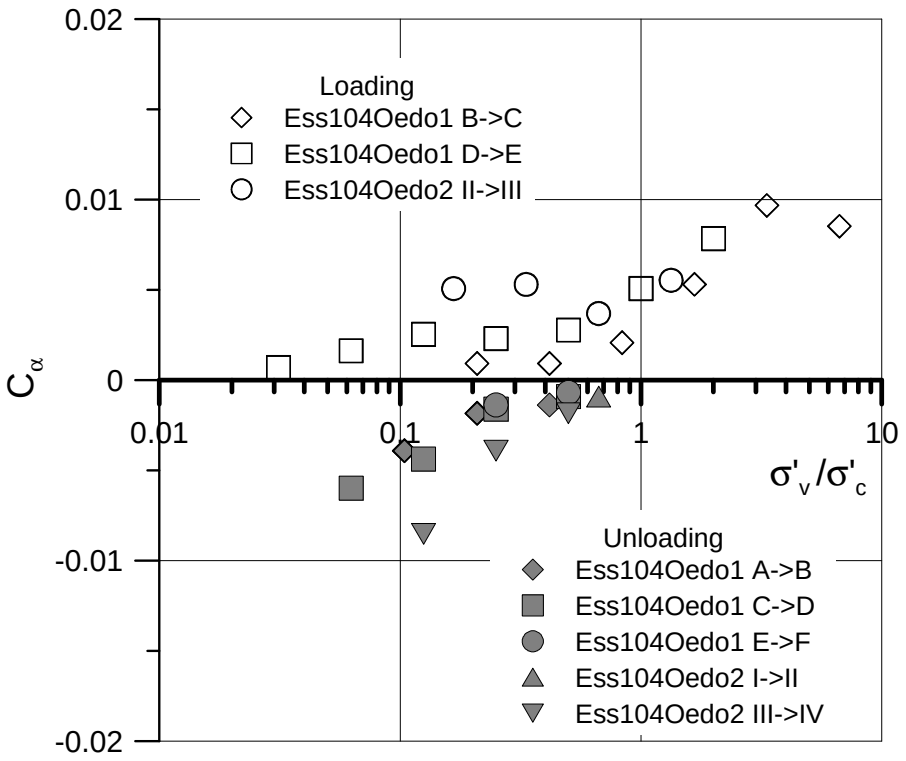
0.02
0.01
0
-0.01
-0.02
0.01
0.1
1
10
C_α
σ'_v/σ'_c
Loading
Ess104Oedo1 B->C
Ess104Oedo1 D->E
Ess104Oedo2 II->III
Unloading
Ess104Oedo1 A->B
Ess104Oedo1 C->D
Ess104Oedo1 E->F
Ess104Oedo2 I->II
Ess104Oedo2 III->IV

(d)

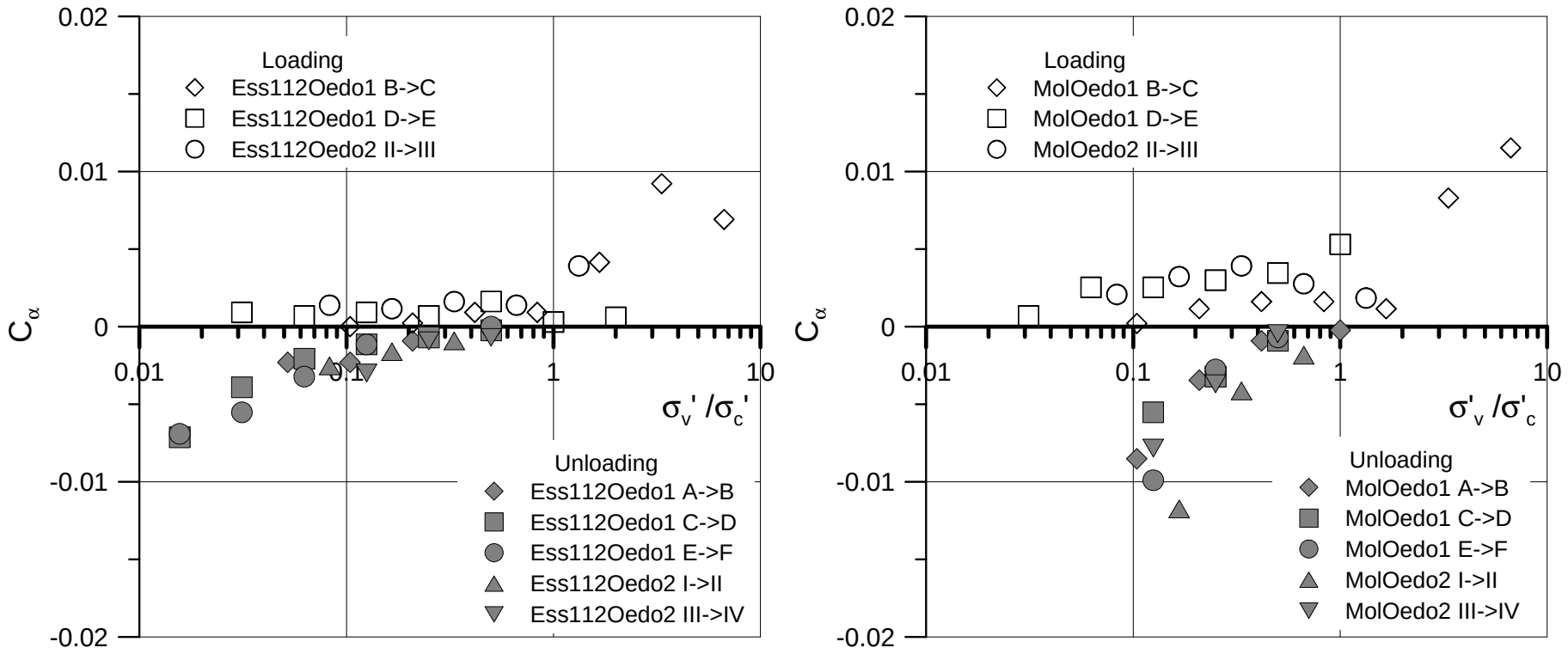

(e) **(f)**

Figure 6. C_α versus stress ratio σ'_v/σ'_c. (a) Core Ess75; (b) Core Ess83; (c) Core Ess96; (d) Core Ess104; (e) Core 112; (f) Core Mol

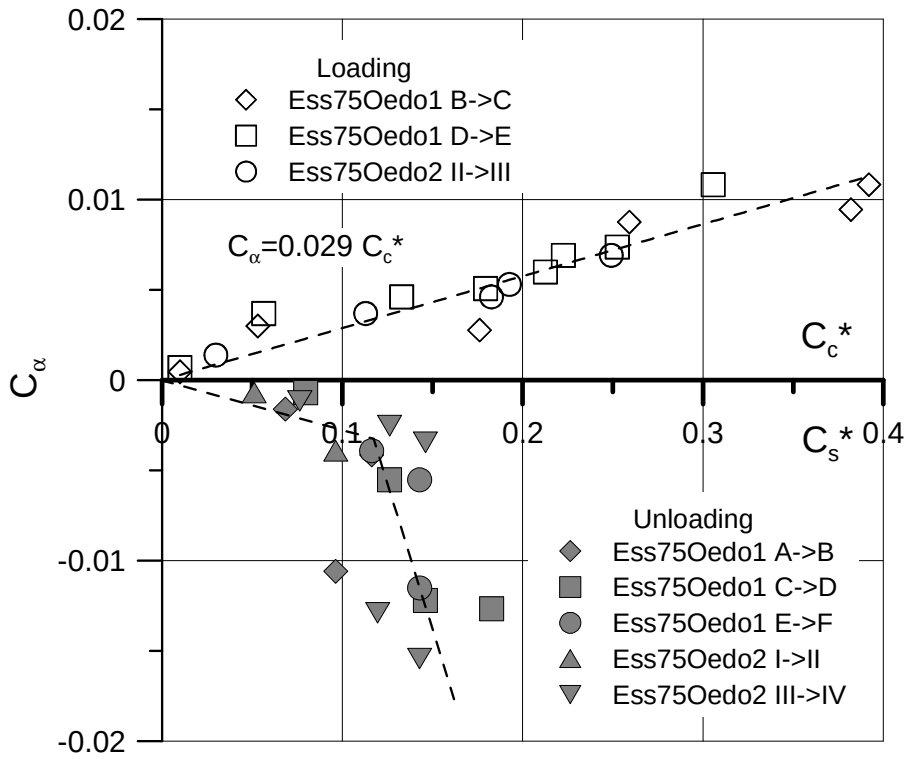
0.02
0.01
0
-0.01
-0.02
C_α
Loading
Ess75Oedo1 B->C
Ess75Oedo1 D->E
Ess75Oedo2 II->III
C_α=0.029 C_c*
C_c*
0
0.1
0.2
0.3
C_s* 0.4
Unloading
Ess75Oedo1 A->B
Ess75Oedo1 C->D
Ess75Oedo1 E->F
Ess75Oedo2 I->II
Ess75Oedo2 III->IV

(a)

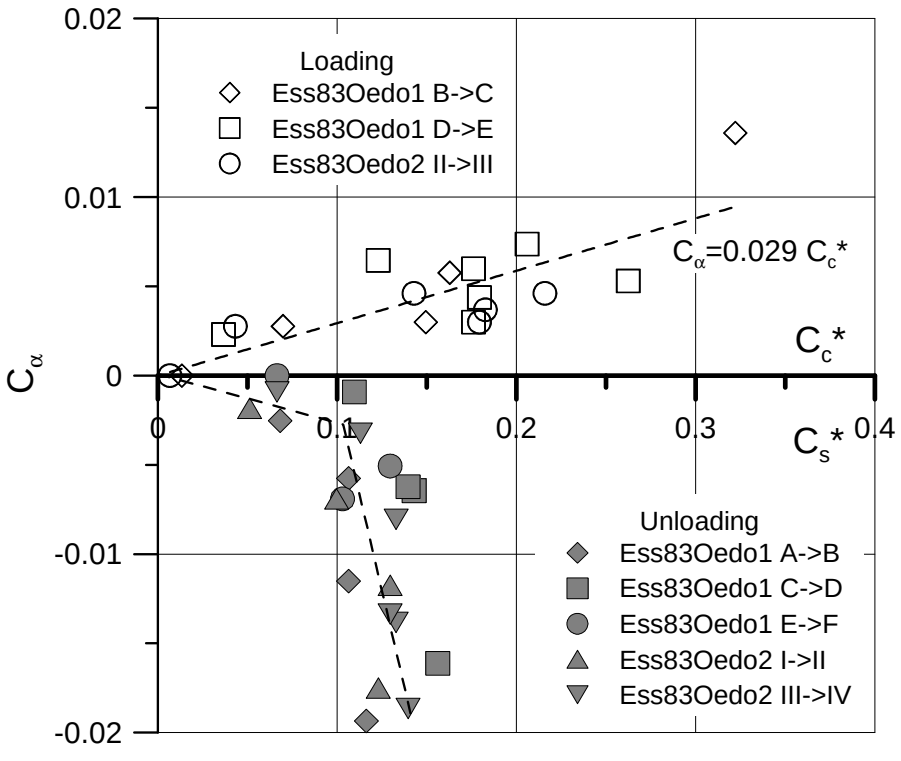
0.02
0.01
0
-0.01
-0.02
C_α
Loading
Ess83Oedo1 B->C
Ess83Oedo1 D->E
Ess83Oedo2 II->III
C_α=0.029 C_c*
C_c*
0
0.1
0.2
0.3
C_s* 0.4
Unloading
Ess83Oedo1 A->B
Ess83Oedo1 C->D
Ess83Oedo1 E->F
Ess83Oedo2 I->II
Ess83Oedo2 III->IV

(b)

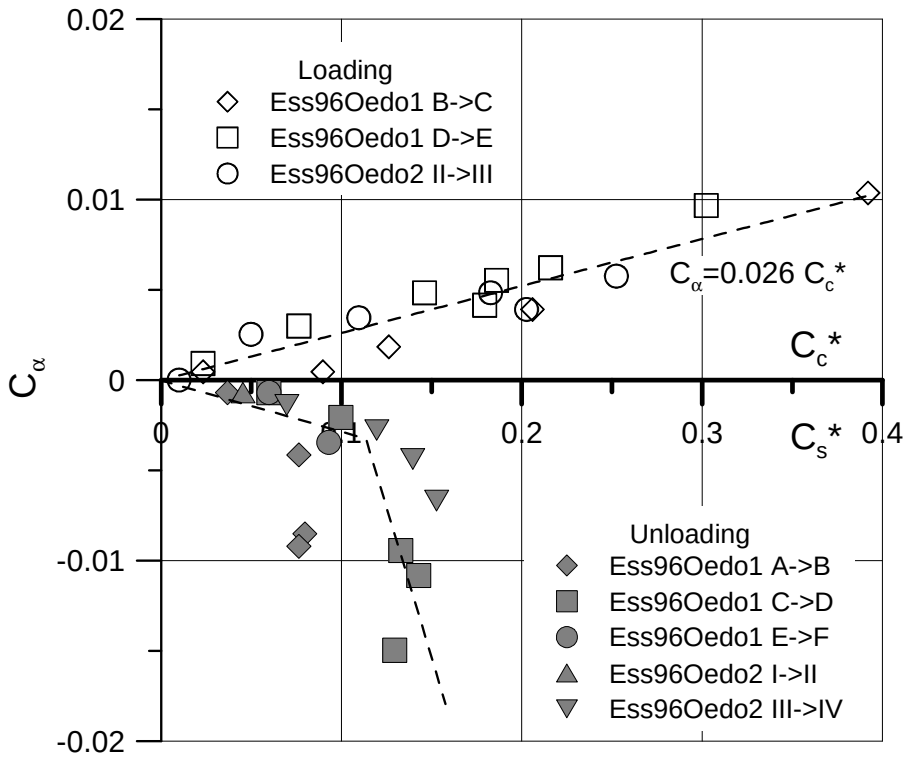
0.02
0.01
0
-0.01
-0.02
0
0.1
0.2
0.3
0.4
C_α
C_c*
C_s*
Loading
Ess96Oedo1 B->C
Ess96Oedo1 D->E
Ess96Oedo2 II->III
C_α=0.026 C_c*
Unloading
Ess96Oedo1 A->B
Ess96Oedo1 C->D
Ess96Oedo1 E->F
Ess96Oedo2 I->II
Ess96Oedo2 III->IV

370

371

(c)

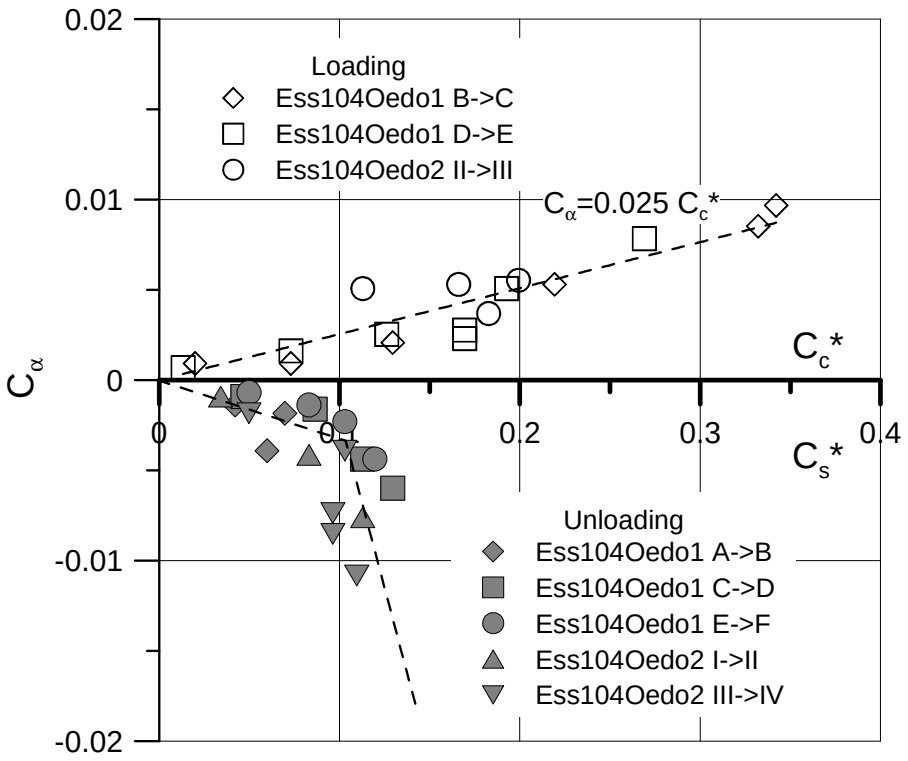
0.02
0.01
0
-0.01
-0.02
0
0.1
0.2
0.3
0.4
C_α
C_c*
C_s*
Loading
Ess104Oedo1 B->C
Ess104Oedo1 D->E
Ess104Oedo2 II->III
C_α=0.025 C_c*
Unloading
Ess104Oedo1 A->B
Ess104Oedo1 C->D
Ess104Oedo1 E->F
Ess104Oedo2 I->II
Ess104Oedo2 III->IV

(d)

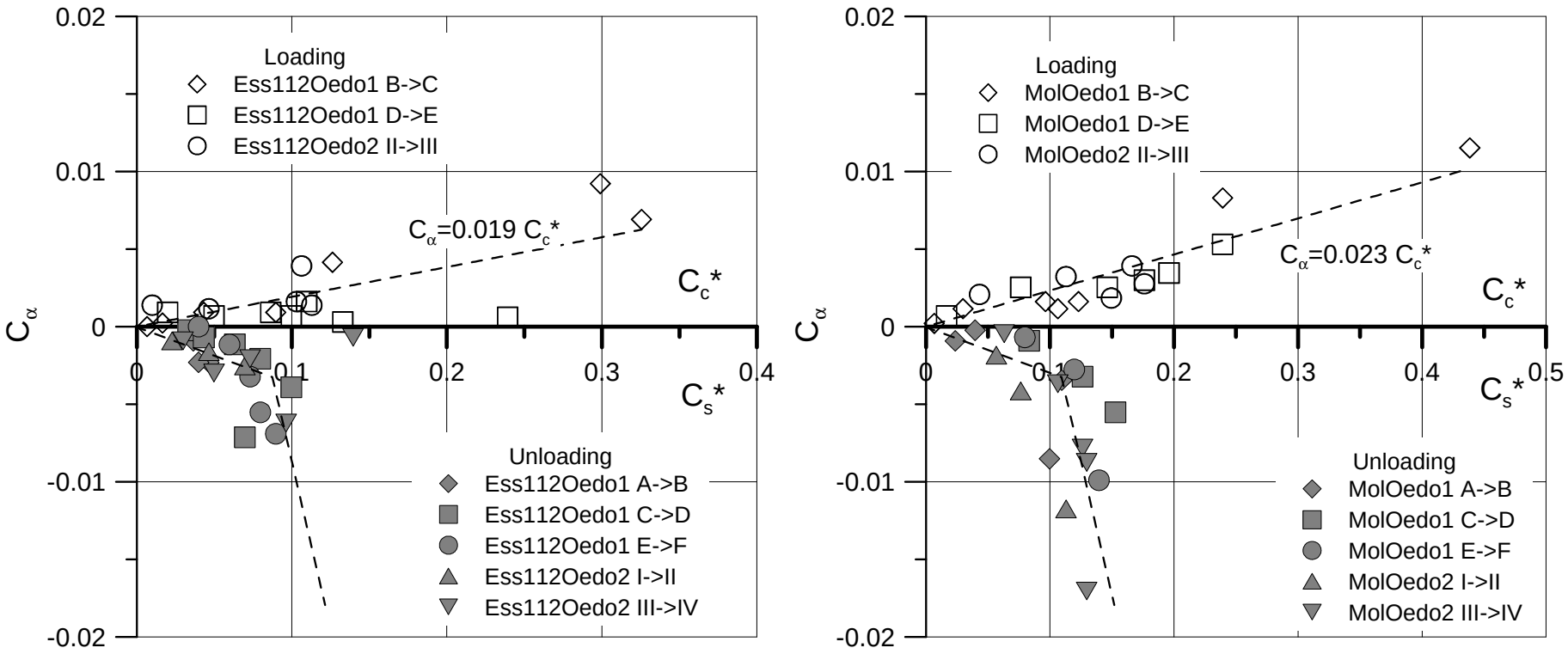

Figure 7. C_α versus C_c* and C_s*. (a) Core Ess75; (b) Core Ess83; (c) Core Ess96; (d) Core Ess104; (e) Core 112; (f) Core Mol

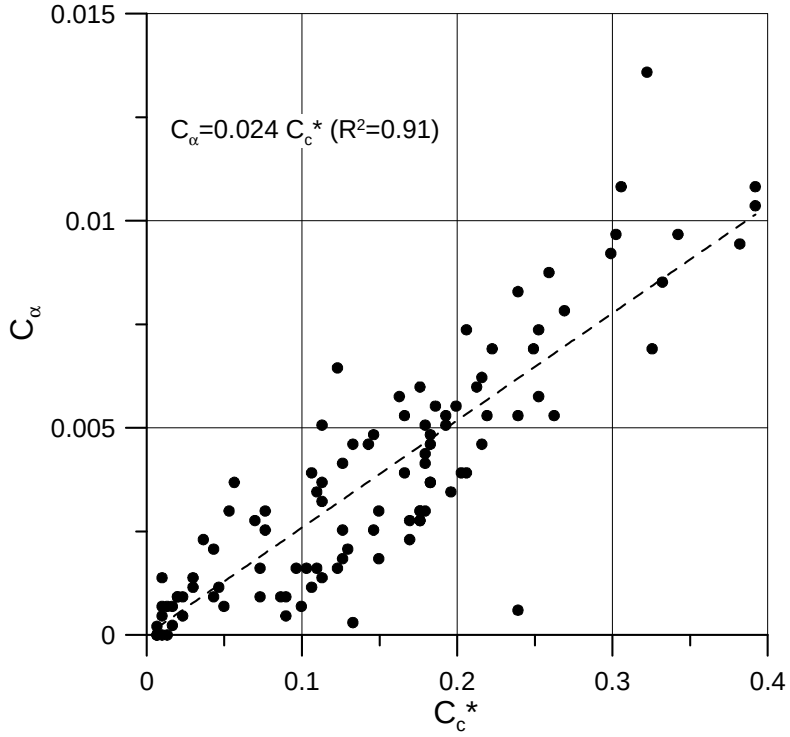

Figure 8. C_α versus C_c*

379

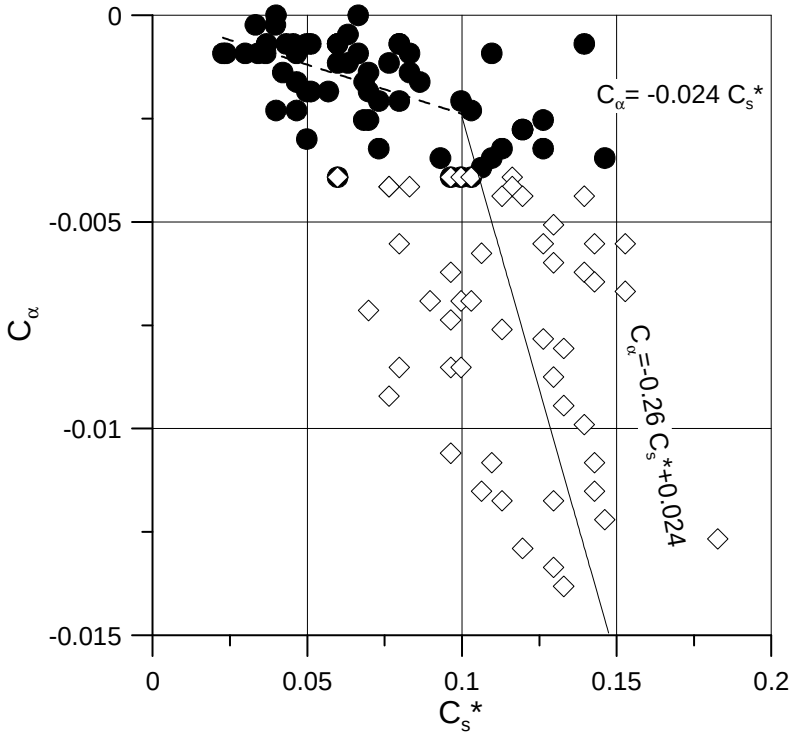

380

381 Figure 9. C_α versus C_s*